JOURNAL OF SOLID STATE CHEMISTRY 31, 285–294 (1980)

An Infrared and Raman Study of New Ionic-Conductor Lithium Glasses

M. IRION* AND M. COUZI

Laboratoire de Spectroscopie Infrarouge, associé au C.N.R.S., Université de Bordeaux I, 351 cours de la Libération,
33045 Talence, Cedex, France

AND A. LEVASSEUR, J. M. REAU, AND J. C. BRETHOUS

Laboratoire de Chimie du Solide du C.N.R.S., Université de Bordeaux I,
351 cours de la Libération, 33405 Talence, Cedex, France

Received October 17, 1978; in revised form April 2, 1979

New vitreous fast ionic conductors in the system B_2O_3–Li_2O–LiCl are described. The conductivity of these glasses increases with the Li_2O and particularly with the LiCl contents. A Raman and infrared study undertaken to elucidate the "structure" of the glasses and the conduction mechanism indicates that the structure consists of a "covalent" boron–oxygen network, in which LiCl is "diluted" without producing detectable interactions with the latter.

Introduction

Storage batteries using superionic conductors as solid electrolytes provide one of the best solutions to the problem of energy storage. A large number of such conductors containing O^{2-} or F^- as the mobile anion, or Li^+, Na^+, or Ag^+ as the mobile cation, have been extensively studied (*1–15*). This paper reports on new materials which have recently been developed at the C.N.R.S. Solid State Chemistry Laboratory at the University of Bordeaux, and in which the ionic conductivity is due to Li^+ ions.[1] The lithium is lighter and gives a larger voltage than the other alkalines. It is the ion best suited for charge transport. Solid solutions $Li_{4+x}B_7O_{12+(x/2)}X$ ($X = Cl$, Br; $0 \leq x \leq 1$) have a high ionic conductivity σ: $Li_4B_7O_{12}Cl$, for instance, has a σ of $10^{-2}\,\Omega^{-1}\,cm^{-1}$ at 300°C (*16*). Furthermore, it has been possible to obtain, from B_2O_3–Li_2O–LiCl melts, glasses which have a large existence region and ionic conductivities comparable to that of $Li_4B_7O_{12}Cl$ (*17*). These glasses are of considerable interest for practical applications (*18*), and they are much easier to work with than crystalline materials.

It was thought for a long time (*19, 20*) that vitreous B_2O_3 consisted of interconnected BO_3 triangles. However, it was recently shown (*21*) by X-ray fluorescence excitation that the structural units, irregularly bonded to one another, are more probably boroxol rings B_3O_6 (Fig. 1). Mozzi and Warren (*21*) also assume that the progressive addition of an alkali oxide to B_2O_3 (up to 20 mole%) causes the appearance of BO_4 tetrahedra, which would partially explain the so-called "boron anomaly."

---

* Present address: Max-Planck-Gesellschaft, D 8046 Garching, R.F.A.

[1] The authors of the C.N.R.S. laboratory would like to acknowledge the support of the D.G.R.S.T.

0022-4596/80/030285-10$02.00/0

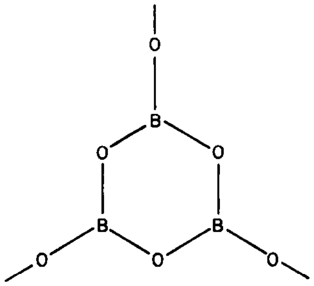

FIG. 1. Schematic representation of a boroxol ring B_3O_6.

To elucidate the conduction mechanism in vitreous borates, one has to know their "structures." Since X-ray diffraction is not the most advantageous for the study of amorphous materials, we have used infrared and Raman spectroscopy in an attempt to determine the short-range structures of borate glasses containing varying amounts of Li_2O and LiCl, with the goal of establishing correlations between the structural and conductivity properties.

Previous Results on Borate Glasses

Vitreous Region of the B_2O_3–Li_2O–LiCl System

The hatched area in Fig. 2 corresponds approximately to the existence region of the glasses (*17*). Outside this region the samples are mixtures of crystalline phases. Point A corresponds to the composition of the crystalline lithium boracite of formula $Li_4B_7O_{12}Cl$ ($=B_2O_3{\cdot}0.43Li_2O{\cdot}0.29LiCl$), and point B to $Li_5B_7O_{12.5}Cl$ ($=B_2O_3.0.57Li_2O{\cdot}0.29LiCl$). According to Levasseur *et al.* (*22*), the structure of Li boracite is built up from a B_2O_3–Li_2O and a LiCl sublattice (Fig. 3). The three-dimensional boron–oxygen framework consists of tetrahedral BO_4 and triangular BO_3 units. Three of the Li atoms form with chlorine a $Cl(Li_I)_6$ sublattice of the anti-ReO_3 type and the fourth, Li_{II}, occupies a tetrahedral site with a 0.25 probability. It is this defect structure that is responsible for the ionic mobility of the Li^+ ions (*16*).

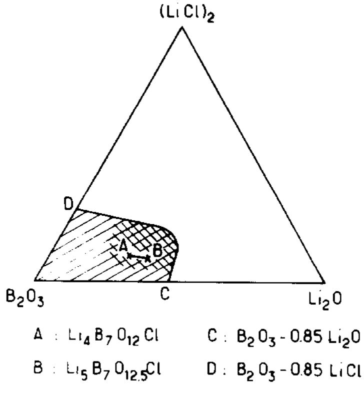

FIG. 2. Vitreous domain of the B_2O_3–Li_2O–LiCl system (*17*) (the cross-hatched area corresponds to high-performance ionic conductors).

Ionic Conductivity

The ionic conductivity of $B_2O_3{\cdot}xLi_2O{\cdot}yLiCl$ vitreous phases has been determined by the complex-impedance method (*17*). This method allows the role of the solid electrolyte to be separated from polarization effects at the electrodes and permits determination of the ohmic

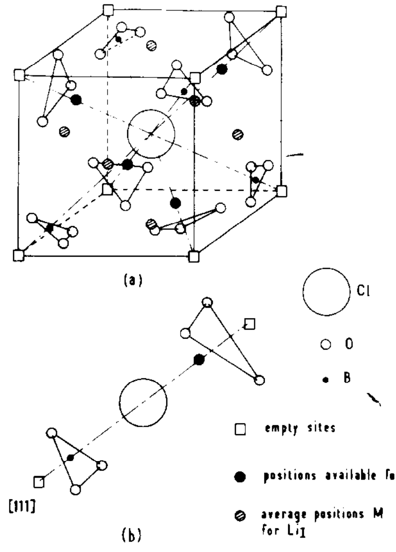

FIG. 3. Boracite structure ($\frac{1}{8}$ of the unit cell).

resistance of a material. Figure 4 shows the temperature dependence of the conductivity of various glasses of definite compositions. These glasses are good ionic conductors, comparable with $Li_4B_7O_{12}Cl$ and $NaAl_{11}O_{17}$; their performance increases with increasing Li_2O and LiCl contents, particularly with the latter (*23*).

To obtain information on short-range order in these glasses, we undertook a Raman and infrared study; the results are presented below. A complete study of ionic conductivity, as a function of Li_2O and LiCl contents, and a concomitant NMR and ESR study are in progress.

Vibrational Spectra

As already mentioned, ir and Raman spectra can be expected to provide information about short-range structure in glasses. Though some similarities with the spectra of the crystal of the same substance often occur (*24*), broad and continuous bands dominate the spectra of glasses. On the other hand, Raman scattering of glasses is very strong compared with the usual second-order Raman scattering in crystals and, for a given substance, is comparable in integrated intensity to the narrow discrete bands which characterize first-order scattering in crystals (*25*). Disorder in a glass has been shown to produce a breakdown in the $\mathbf{K} = 0$ Raman selection rule and all modes of vibration are allowed to participate in the scattering. This led Shuker and Gamon to conclude (*25*) that Raman scattering in disordered materials is first order and is closely related to the vibrational density of states. The total observed scattering intensity, $I_{obs}(\omega)$, of the Stokes component is given by (*25*):

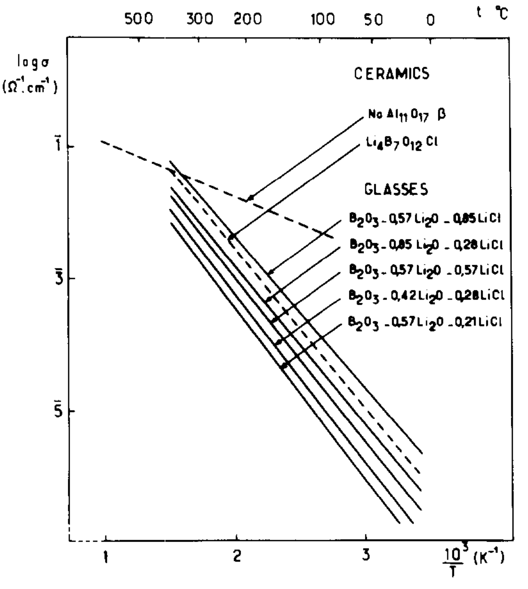

FIG. 4. Temperature dependence of electrical conductivity for some glasses of definite composition in the B_2O_3–Li_2O–LiCl system and for $Li_4B_7O_{12}Cl$ and β-$NaAl_{11}O_{17}$ (*9*).

$$I_{obs_{(\omega)}} = (\hbar/2\omega)[n(\omega)+1]\sum_{b} C_b g_b(\omega), \tag{1}$$

where $g_b(\omega)$ is the density of states for a vibrational band b; C_b represents the derived polarizability tensor elements, which are assumed to be frequency independent for a given band b but to depend on the band considered; and $n(\omega) = [\exp(\hbar\omega/KT) - 1]^{-1}$ is the Bose Einstein population factor.

No systematic study of the vibrational spectra of lithium borate glasses (systems B_2O_3–Li_2O and B_2O_3–Li_2O–LiCl) has been reported so far. However, the amorphous systems B_2O_3–xNa_2O and B_2O_3–xK_2O have been recently investigated by Konijnendijk (*26*) and by Bril (*27*); the vibrational spectra of these glasses have been compared with those of numerous appropriate crystalline compounds (*26–28*). The results have confirmed that vitreous B_2O_3 is built up from a random network of boroxol rings, B_3O_6 (Fig. 1). On adding up to about $x \simeq 0.25$ Na_2O or K_2O to B_2O_3 glass, the appearance of new features was observed and assigned to the presence of triborate groups (*27*) (Fig. 5). However, from a comparison of melting-point depression (*29*) and NMR (*30*) measurements, Konijnendijk concluded that

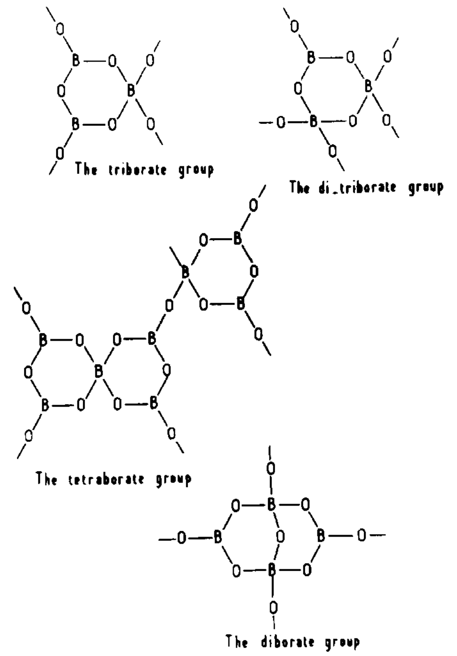

FIG. 5. Some structural units of crystalline and amorphous alkali borates.

the triborate groups were in fact incorporated in the more complex tetraborate units (*28*).

In the composition range between $x = 0.25$ and $x = 0.54$, the tetraborate groups are progressively replaced by diborate groups as the alkali content increases. At $x = 0.50$ a small number of isolated metaborate rings, $B_3O_6^{3-}$, is probably also present (*28*).

Experimental

The glass samples were cut with diamond tools into parallelepipeds of about $10 \times 10 \times 5$ mm^3 and the surfaces carefully polished. All samples of compositions $B_2O_3 \cdot xLi_2O$ and $B_2O_3 \cdot xLi_2O \cdot yLiCl$ were colorless and, after polishing, completely transparent. Because of the hygroscopicity of powdered compounds containing B_2O_3, the infrared reflection was measured on freshly polished surfaces of bulk material.

Raman scattering experiments were performed with a Coderg T-800 triple monochromator instrument coupled with a Spectra Physics Model 171 argon ion laser. We used the emission lines at either 488.0 or 514.5 mm with an incident power of less than 1.5 W. Typical slit widths were about 3 cm^{-1}. The detection was made with an EMI 9558 A cooled photomultiplier, coupled with a dc amplifier.

In the far-infrared region, between 10 and 300 cm^{-1}, several spectra were studied using a Model FIR 30 Polytec Fourier-transform interferometer. Spectra in the middle-infrared region, 250–4000 cm^{-1}, were recorded with a Model 180 Perkin–Elmer double-beam spectrophotometer equipped with a reflection unit which allowed measurements at an incidence angle of about 11°.

Results and Discussion

Pure B_2O_3

Pure boron oxide glass is characterized by a strong, rather narrow ($\Delta\nu_{1/2} \approx 10$ cm^{-1}) Raman peak at 806 cm^{-1} and by infrared reflection maxima at 656, 1276 (very strong), and 1492 cm^{-1}. The strongly polarized Raman peak at 806 cm^{-1} has been assigned by Kristiansen and Krogh-Moe (*31*) to the trigonal deformation of the boroxol ring (Fig. 6). However, Bril (*27*) has recently advanced arguments (based on a comparison with crystalline sodium metaborate $Na_3B_3O_6$) in favor of assigning the 806-cm^{-1} peak to the symmetric ring breathing vibration of the boroxol ring (Fig. 6). On the other hand,

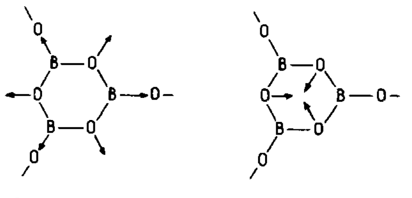

FIG. 6. The two possible symmetric vibrations of the boroxol ring responsible for the 806-cm^{-1} Raman peak.

the strong infrared band at 1276 cm^{-1} and the shoulder at 1492 cm^{-1} can be assigned (*32, 33*) to B–O stretching vibrations, whereas the weak band at 656 cm^{-1} may correspond to the bending motion of the B–O–B centers within the network (*32*).

Binary System B_2O_3–xLi_2O

Raman spectra. The addition of Li_2O to B_2O_3 produced significant changes in the Raman spectrum. In particular, the progressive disappearance of the 806-cm^{-1} peak was accompanied by a rapid increase in the intensity of a new strong, polarized peak at 780 cm^{-1}. At $0.05 \leq x \leq 0.25$ both peaks are present in the spectra of the $B_2O_3 \cdot xLi_2O$ glasses, while at $x = 0.33$ the 806-cm^{-1} peak had completely vanished. Further addition of Li_2O, up to the boundary of the glass region, resulted in a continuous broadening of the 780-cm^{-1} peak and a slow shift of its frequency to 772 cm^{-1} at $x = 0.56$ (Fig. 7). Similar trends in the spectra of amorphous B_2O_3–Na_2O and B_2O_3–K_2O have previously been reported by Bril (*27*) and by Konijnendijk (*28*).

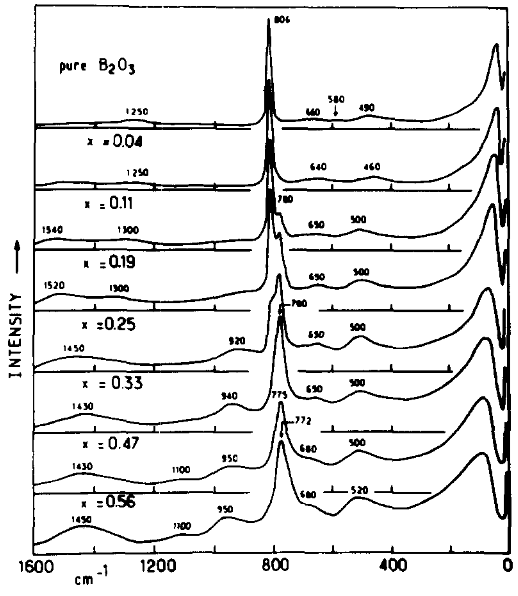

FIG. 7. Raman spectra (I_{vv}) of B_2O_3 and glasses of definite B_2O_3–xLi_2O composition.

As shown by NMR (*34*), on introducing an alkali oxide at concentrations of up to $x = 0.25$ into vitreous B_2O_3 (B_2O_3–xLi_2O), the coordination number of some of the boron atoms in the boroxol rings changes from three to four. A BO_4 unit can be incorporated in a boroxol ring in various ways (*27*). The simplest hypothesis is to imagine that the boroxol rings are progressively replaced by triborate groups (Fig. 5). If this is so, at $x = 0.33$ all boroxol rings must be transformed, for reasons of stoichiometry, into triborate groups. Indeed, the 806-cm^{-1} peak, characteristic of boroxol rings, vanishes at this composition. Following Bril (*27*), we assign the new 780-cm^{-1} Raman band to the symmetric breathing vibration of a six-membered borate ring with one BO_4 group, i.e., of triborate groups (Fig. 5). Bril, however, in the case of sodium borate glasses, argued that structural groups with a higher content of BO_4 units are also present in this concentration range, e.g., diborate, ditriborate, or dipentaborate groups (Fig. 5). In contrast, in the case of potassium–borate glasses, Konijnendijk (*28*) concluded that tetraborate groups are predominant at these concentrations (i.e., structural groups with fewer BO_4 units than the triborate). Note, however, that at $x = 0.25$ (the tetraborate concentration) boroxol rings are still present in the lithium–borate glasses (Fig. 7), whereas they should have been completely transformed if only tetraborate groups are formed. Thus, the assignment of the 780-cm^{-1} line to the presence of predominant triborate groups seems to us a reasonable hypothesis, even though more complicated structural units containing BO_4, such as tetraborate groups, may turn out to be also responsible for this peak.

On further addition of Li_2O ($0.33 < x < 0.56$), the number of BO_4 units relative to BO_3 units increases. Again, several combinations are possible, e.g., formation of diborate or ditriborate groups (Fig. 5), as suggested by comparing the Raman spectra of glasses in this composition range with those of crystalline Li_2O -B_2O_3 and K_2O–B_2O_3 (*28*) which contain such structural units. Then the small frequency shift of the main peak in the spectra of B_2O_3–$x Li_2O$ ($0.33 < x < 0.56$) glasses from 780 to 772 cm^{-1} might be due to the formation of diborate and/or ditriborate groups. Konijnendijk (*28*) argued that essentially diborate groups are present in the corresponding concentration range of B_2O_3–$x K_2O$ glasses. There is, however, a serious difficulty in the assignment of the 772-cm^{-1} line to diborate groups: crystalline Li_2O–$2B_2O_3$ and ZnO–$2B_2O_3$ both contain diborate groups only (*35*, *36*), but their Raman spectra are drastically different (*28*). In particular, $ZnO \cdot 2B_2O_3$ does not present strong features around 770 cm^{-1}, whereas Li_2O–$2B_2O_3$ does, and it is not at all obvious that solely the influence of the Zn^{2+} on the spectrum of the diborate group can account for such strong differences in this range of frequency. Thus in the absence of further structural and spectroscopic investigations, we assign the 772-cm^{-1} peak in the glasses B_2O_3–$x Li_2O$ to the presence of ditriborate and possibly of diborate groups.

We also found in our spectra (Fig. 7) weak and, compared with the peaks at 806, 780, and 772 cm^{-1}, very broad bands at about 500, 650–700, 950, and 1400–1500 cm^{-1}, similar to those observed in the Raman spectra of the corresponding sodium and potassium glasses (*28*). No attempt has been made to analyze their origin because of the lack of additional information. However, following the theoretical considerations of vitreous networks developed by Brawer (*24*), the strong and relatively narrow peaks at 806 and 780–772 cm^{-1} should correspond to localized Raman modes. This agrees with the assignment of these peaks to ring breathing vibrations (*27*). The broad and poorly defined features reported above more likely correspond to extended vibrations resulting from vibrational coupling among a large number of atoms in the glass (*24*) rather than to a single mode.

Finally, in the 26- to 88-cm^{-1} region, near the exciting line, a large, broad peak is observed; in contrast to all the other Raman features, it is only weakly polarized. This peak, which in pure B_2O_3 occurs at 26 cm^{-1}, shifts in the $B_2O_3 \cdot x Li_2O$ glasses progressively with increasing Li_2O contents to 88 cm^{-1} at $x = 0.56$. The corresponding low-frequency feature in the spectra of B_2O_3–Na_2O glasses has been assigned by Bril (*27*) to a band of modes due to translational and librational motions of network fragments. Bril has also related the frequency of the observed maximum to the size of these fragments. This line of argument has to be viewed with some caution because of the population effect at low frequency (*25*).

Indeed, a similar peak appears in most glasses and is caused by the competition between the decreasing density of vibrational states and the increasing thermal population that occurs as the vibrational frequencies decrease toward zero. Thus, it is necessary to consider the "reduced" Raman intensity (*25*), which is defined as

$$\begin{aligned} I_{\mathrm{red}}(\omega) &= \omega |n(\omega) + 1|^{-1} I_{\mathrm{obs}}(\omega) \\ &= (\hbar/2) \sum_b C_b g_b(\omega), \end{aligned} \tag{2}$$

where $n(\omega)$, C_b, and $g_b(\omega)$ are the same as in Eq. (1). I_{red} is now more closely related to the frequency distribution, and its frequency dependence is shown in Fig. 8. The strong peak at 26–88 cm^{-1} of the I_{vv} spectra of B_2O_3–$x Li_2O$ ($0.33 < x < 0.56$) glasses almost disappeared: in the reduced I_{vv} spectra, only a broad, weak shoulder persists at low frequency (Fig. 8). Exceptionally, the I_{vv} spectrum of pure B_2O_3 exhibits a maximum at about 140 cm^{-1} and a shoulder near 90 cm^{-1}. However, a maximum is always present in the reduced I_{vh} spectra for all compositions, and it shifts from about

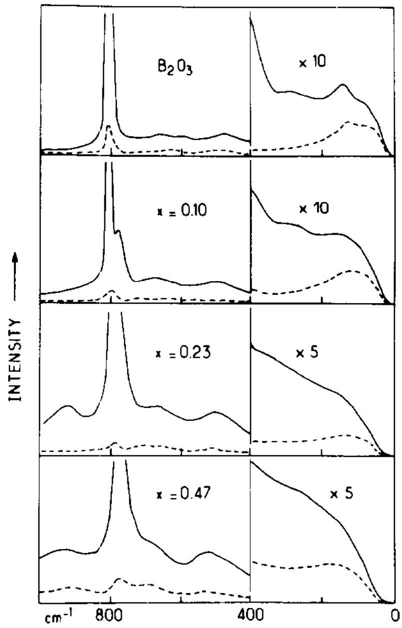

FIG. 8. The reduced Raman spectra in the region of 0–1000 cm^{-1} for B_2O_3–$x Li_2O$ glasses. (——)I_{vv}; (· · · ·)I_{vh}.

130 cm^{-1} at $x = 0$ to about 180 cm^{-1} at $x = 0.47$. This maximum now appears more likely to correspond to a maximum in the frequency distribution and to the translational and librational motions of network fragments. Also, no localized vibrational mode involving the alkaline ions can be identified in the spectra of B_2O_3–$x Li_2O$. It is possible that such vibrations involving the Li^+ ions are included in this low-frequency distribution and are partially responsible for the frequency shift of the maximum observed on the addition of Li_2O.

Infrared reflection spectra. Infrared reflection spectra of $B_2O_3 \cdot x Li_2O$ glasses in general show three mean maxima which, for $0 < x < 0.33$, shift slowly in frequency and relative intensity with x (Fig. 9). The three peaks at 1492, 1276, and 656 cm^{-1} in the spectrum of pure B_2O_3 are progressively replaced by peaks at 1376, 920, and 676 cm^{-1}, respectively. In particular, the strong B_2O_3 band at 1276 cm^{-1} has nearly disappeared at $x = 0.33$, which is consistent with the assignment of this frequency to a B–O stretching vibration of the boroxol ring.

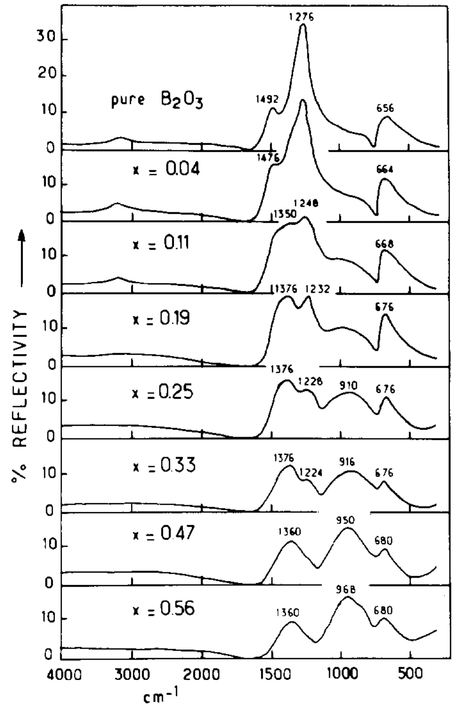

FIG. 9. Infrared reflection spectra of B_2O_3 and $B_2O_3 \cdot x Li_2O$ glasses of definite compositions.

The spectral evolution is again similar to that reported for $B_2O_3 \cdot x Na_2O$ glasses (*28*) and may be compared with the above evolution in the Raman spectra, where the B_2O_3 features also disappear at $x = 0.33$. A detailed assignment of the infrared reflection maxima is not at all obvious, since the observed broad bands are certainly due to the overlap of absorptions arising from several vibrational modes. However, comparison with the infrared spectra of appropriate crystalline borates suggests, in a qualitative fashion, that up to $x = 0.33$ the observed spectral changes are due to the formation of primarily triborate and tetraborate groups and to the gradual disappearance of boroxol rings. In the composition range $0.33 < x < 0.56$, ditriborate and possibly diborate groups are assumed to be present. This conclusion is again slightly different from that given by Konijnendijk from an infrared study of sodium–borate glasses (*26*, *28*), in which diborate groups have been determined to be predominant.

Ternary System $B_2O_3 \cdot xLi_2O \cdot yLiCl$

The Raman scattering and infrared reflection spectra of $B_2O_3 \cdot xLi_2O \cdot yLiCl$ glasses of various compositions are shown in Figs. 10–12. No new features are detected compared with the spectra of the $B_2O_3 \cdot xLi_2O$ glasses (Figs. 7 and 9); for a given x, the spectra of the binary and ternary compounds are nearly identical. Only a slight difference is found in the low-frequency range of the Raman spectra: The relative intensity of the 0- to 400-cm^{-1} band increases with the LiCl concentration, but no striking modification of its shape or of the position of its maximum is observed. The far-infrared reflectivity also increases with increasing LiCl content, but no maximum in the reflection spectra can be detected between 15 and 500 cm^{-1}. Thus, as for the binary B_2O_3–xLi_2O glasses, no localized vibrations involving the Li^+ ions can be detected in the ternary compositions. The relative increase in the intensity of the low-

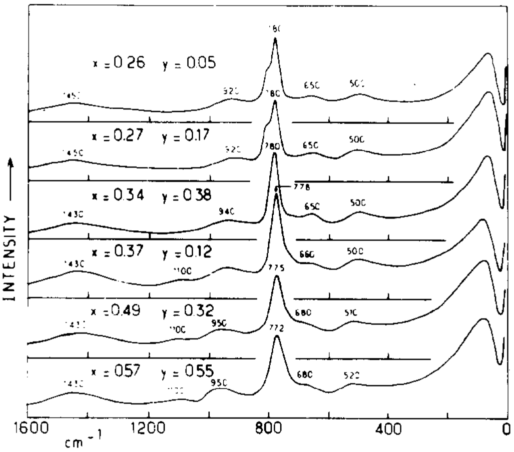

FIG. 10. Raman spectra of $B_2O_3 \cdot xLi_2O \cdot yLiCl$ glasses of definite compositions.

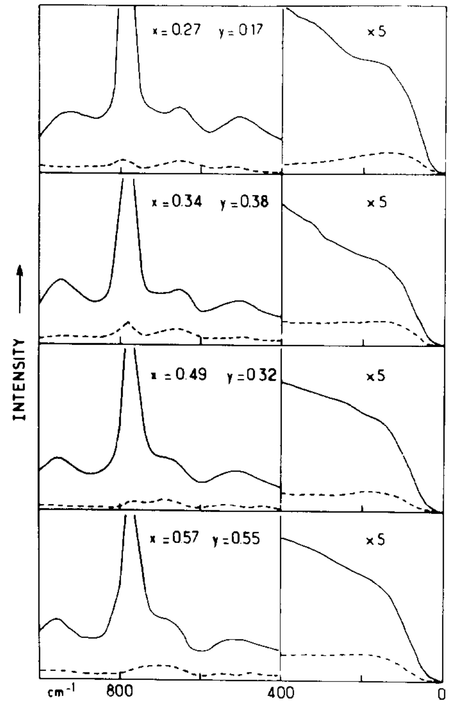

FIG. 11. The reduced Raman spectra in the region of 0–1000 cm^{-1} for $B_2O_3 \cdot xLi_2O \cdot yLiCl$ glasses. (——) I_{vv}; (· · · ·) I_{vh}.

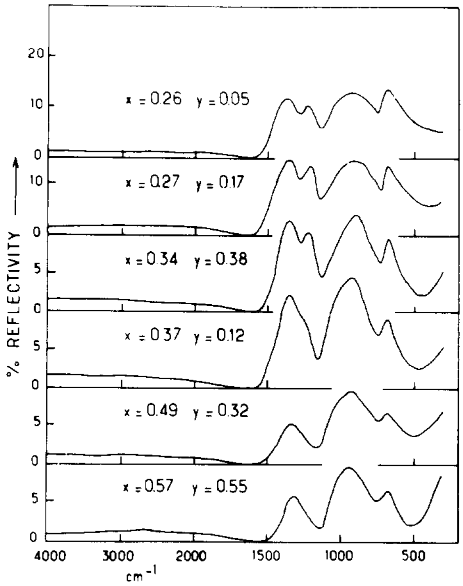

FIG 12. Infrared reflection spectra of $B_2O_3 \cdot xLi_2O \cdot yLiCl$ glasses of definite compositions.

frequency distribution on the addition of LiCl again suggests that such vibrations contribute to the broad scattering observed at 0–400 cm^{-1}. It may thus be concluded that the addition of LiCl does not produce any major modification in the vitreous boron–oxygen network, and the interpretation of the vibrational spectra of simple borate glasses may be extended to the spectra of the conducting ternary compositions.

No similarity could be found between the Raman spectrum of the crystalline boracite $Li_4B_7O_{12}Cl$ ($=B_2O_3{\cdot}0.43Li_2O{\cdot}0.30LiCl$) (Fig. 13) and that of a glass nearest to the boracite composition (Fig. 10). This result, which is not very surprising, is compatible with the overall interpretation of our findings. The tri- and tetraborate groups, and the diborate groups, present in vitreous material of corresponding compositions, have not been found in the crystalline boracite.

Conclusions

Comparisons of the Raman scattering and infrared reflection spectra of B_2O_3–$xLi_2O{\cdot}yLiCl$ and B_2O_3–xLi_2O glasses give a clear indication of the existence of a "covalent" boron–oxygen network whose structure depends on the relative concentrations of B_2O_3 and Li_2O. In this boron–oxygen "lattice" LiCl is apparently "diluted" without producing strong interactions, as they have not been detected by vibrational spectroscopy even for the relatively high LiCl concentration of $y = 0.55$.

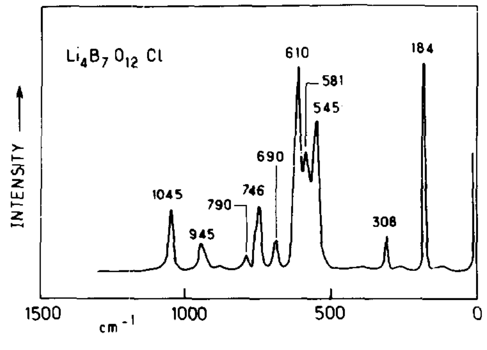

FIG. 13. Raman spectrum of a single crystal of boracite, $Li_4B_7O_{12}Cl$ ($=B_2O_3{\cdot}0.43Li_2O{\cdot}0.30LiCl$).

References

1. CH. DEPORTES, G. ROBERT, AND M. FORESTIER, *Electrochim. Acta* **16**, 1003 (1971).
2. A. HAMMOU, CH. DEPORTES, AND G. ROBERT, *J. Chem. Phys.* **7–8**, 1162 (1971).
3. J. M. REAU, C. LUCAT, G. CAMPET, J. CLAVERIE, AND J. PORTIER, *Electrochim. Acta* **22**, 761 (1977).
4. C. LUCAT, PH. SORBE, J. PORTIER, J. M. REAU, P. HAGENMULLER, AND J. GRANNEC, *Mat. Res. Bull.* **12**, 145 (1977).
5. H. Y. P. HONG, *Mat. Res. Bull.* **13**, 117 (1978).
6. B. E. TAYLOR, A. D. ENGLISH, AND T. BERZINS, *Mat. Res. Bull.* **12**, 171 (1977).
7. I. D. RAISTRICK, CHUN HO, AND R. A. HUGGINS, *J. Electrochem. Soc.* **123**, 10, 1469 (1976).
8. R. D. SHANNON, B. E. TAYLOR, A. D. ENGLISH, AND T. BERZINS, *Electrochim. Acta* **22**, 783 (1977).
9. M. S. WHITTINGHAM AND R. A. HUGGINS, *J. Chem. Phys.* **54**, 414 (1971).
10. J. P. BOILOT, J. THERY, AND R. COLLONGUES, *Mat. Res. Bull.* **8**, 1143 (1973).
11. J. P. BOILOT, A. KAHN, J. THERY, AND R. COLLONGUES, *J. Chim. Phys.* **74**, 7–8, 844 (1977).
12. J. B. GOODENOUGH, H. Y. P. HONG, AND J. A. KAFALAS, *Mat. Res. Bull.* **11**, 203 (1976).
13. L. TRICHET AND J. ROUXEL, *Mat. Res. Bull.* **12**, 345 (1977).
14. H. WIEDESICH AND S. GELLAR, "The Chemistry of Extended Defects in Nonmetallic Solids" (L. Eyring and M. O'Keefe, Eds.), p. 629, North-Holland, Amsterdam (1970).
15. A. KVIST AND A. JOSEFSON, *Z. Naturforsch.* **23A**, 625 (1968).
16. B. CALES, A. LEVASSEUR, C. FOUASSIER, J. M. REAU, AND P. HAGENMULLER, *Solid State Commun.* **24**, 323 (1977).
17. A. LEVASSEUR, B. CALES, J. M. REAU, AND P. HAGENMULLER, *C. R. Acad. Sci.* **285**(C), 471 (1977).
18. J. M. REAU, A. LEVASSEUR, C. FOUASSIER, B. CALES, AND P. HAGENMULLER, Brevet D.R.M.E. France No. 7711376.
19. B. E. WARREN, *J. Amer. Ceram. Soc.* **24**, 256 (1941).
20. B. E. WARREN, J. Appl. Phys. **13**, 602 (1942).

21. R. L. Mozzi and B. E. Warren, *J. Appl. Cryst.* **3**, 251 (1970).

22. A. Levasseur, D. J. Lloyd, C. Fouassier, and P. Hagenmuller, *J. Solid State Chem.* **8**, 318 (1973).

23. A. Levasseur, B. Cales, J. M. Reau, and P. Hagenmuller, *Mat. Res. Bull.* **13**, 205 (1978).

24. S. Brawer, *Phys. Rev.* **B11**, 3173 (1975).

25. R. Shuker and R. W. Gamon, *in* "Proceedings 2nd International Conference on Light Scattering in Solids" p. 334, Flammarion Sciences, Paris (1971).

26. W. L. Konijnendijk and J. M. Stevels, *J. Noncrystal. Solids* **18**, 307 (1975).

27. T. W. Bril, *Philips Res. Rep.*, Suppl. **2** (1976).

28. W. L. Konijnendijk, *Philips Res. Rep.* Suppl. **1** (1975).

29. J. Krogh-Moe, *Phys. Chem. Glasses* **3**, 101 (1962).

30. C. Rhee and P. J. Bray, *Phys. Chem. Glasses* **12**, 165 (1971).

31. L. A. Kristiansen and J. Krogh-Moe, *Phys. Chem. Glasses* **2**, 96 (1968).

32. A. S. Tenney and J. Wong, *J. Chem. Phys.* **56**, 5516 (1972).

33. J. Krogh-Moe, *Phys. Chem. Glasses* **6**, 46 (1965).

34. P. J. Bray and G. O'Keefe, *Phys. Chem. Glasses* **4**, 37 (1963).

35. J. Krogh-Moe, *Acta Crystallogr.* **B24**, 179 (1968).

36. M. Martinez-Ripoll, S. Martinez-Carrera, and S. Garcia-Blanco, *Acta Crystallogr.* **B27**, 672 (1971).